Available online at www.sciencedirect.com
SCIENCE DIRECT®
Analytica Chimica Acta 493 (2003) 69–81
ANALYTICA CHIMICA ACTA
www.elsevier.com/locate/aca

Determination of doxorubicin in human plasma by excitation–emission matrix fluorescence and multi-way analysis☆

Marcello G. Trevisan, Ronei J. Poppi*

Instituto de Química, Universidade Estadual de Campinas, Caixa Postal (CP) 6154, 13083-970 Campinas, São Paulo, Brazil

Received 7 October 2002; received in revised form 3 July 2003; accepted 4 July 2003

Abstract

Direct determination of doxorubicin (DXR), a cytotoxic anthracycline antibiotic, in human plasma was accomplished based on excitation–emission matrix (EEM) fluorescence measurements and multi-way chemometric methods based on parallel factor analysis (PARAFAC) and N-PLS. Several different procedures, such as residual analysis, core consistency diagnostic (CONCORDIA) and split-half analysis were employed to determine the correct number of factors in PARAFAC. These procedures converged to a choice of two factors, attributed to DXR and to the sum of two fluorescence species present in the plasma. Sample PARAFAC loadings were employed to build a regression model against concentration, resulting in a RMSECV of 0.060 $\mu g\,ml^{-1}$. N-PLS using two factors produced a RMSECV of 0.045 $\mu g\,ml^{-1}$. Figures of merit (FOM), such as sensitivity (SEN), selectivity (SEL) and limit of detection (L_D) were determined for both PARAFAC and N-PLS.

Keywords: Doxorubicin; Anthracycline; PARAFAC; Human plasma; Excitation–emission fluorescence; Drugs

1. Introduction

Doxorubicin (DXR) or adriamicin is a cytotoxic anthracycline antibiotic widely employed in clinical practice, showing activity against a wide range of human neoplasms, including a variety of solid tumors. Doxorubicin, first isolated in the 60's [1], is an amphiphilic molecule that has a fluorescent naphthacenedione nucleus linked at C7 to a hydrophilic aminoglycosidic side chain. Its chemical structure [2] is shown in Fig. 1.

The highlight in determination and monitoring of anthracyclines is based on their toxic effects commonly observed after long-term treatment, such as the toxicity to the myocardium, disturbance in hair growth and spermatogenic suppression [3]. The clinical efficacy of doxorubicin is related to its actual concentration in the tumor tissue, however the metabolism of the drug and consequently its concentration in vivo varies from patient to patient and has to be evaluated for each one [4]. Consequently, several methodologies have been developed for the determination of doxorubicin in biological fluids using high performance liquid chromatography [5–8], capillary electrophoresis [9–11], UV-Vis [12] and Raman [13] spectroscopies. In recent review, Zagotto et al. [4] report news developments on the determination of anthracyclines, using figures of merit (FOM) for validation and comparison

☆ Presented at CAC 2002, Seattle, WA, USA, 22–26 September 2002.

* Corresponding author. Tel.: +55-1937883126; fax: +55-1937883023.
E-mail address: ronei@iqm.unicamp.br (R.J. Poppi).

0003-2670/$ – see front matter © 2003 Elsevier B.V. All rights reserved.
doi:10.1016/S0003-2670(03)00864-X

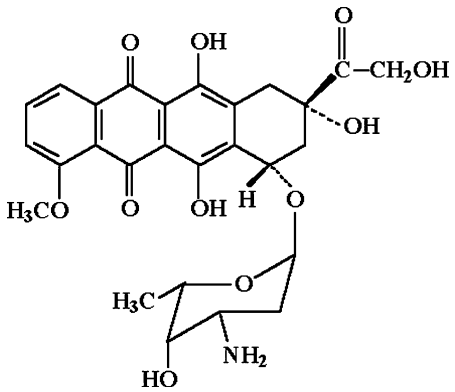

Fig. 1. Chemical structure of doxorubicin.

between the several methods. Currently, figures of merit applied in multi-way determination are scarce, however this is an important process for comparison and to validate methodologies.

Determination of DXR in biological fluids has only been reported using separations methodologies, but these are relatively time consuming and laborious. Direct fluorescence measurement in plasma can be an attractive alternative, due to its high sensitivity (SEN) and selectivity (SEL), allied to fast and clean spectra acquisition, since DXR has a fluorophore group.

However, a method based on direct fluorescence measurements of DXR in plasma, which is the case for real samples, using univariate calibration at a single emission wavelength may be biased by the native fluorescence of the samples, and bad results will be obtained. Human plasma is composed of a variety of components and some of them make significant contributions to the overall fluorescence. The fluorescence of plasma can be split into two parts; one part comprises the highly fluorescent ultraviolet region, basically due the strong fluorescence of tryptophan. The other part comprises the near-ultraviolet and visible part of spectrum, due to many components, like nicotinamide adenine dinucleotide (NAD) and its phosphate, riboflavin, bilirubin and others [14]. These components present into the plasma can significantly change from individual to individual, and the difference in the fluorescence profile can be due to pH variation, intrinsic characteristics of each individual or even the bad performance of certain organs, as verified by Madhuri et al. [15] who related the differences between normal and liver-diseased subjects from native fluorescence characteristics of blood plasma.

Also first-order calibration methods such as partial least squares (PLS) [16] are difficult to be used in this case, since they require that all detectable species (analytes and interferents) must be present in both standards for calibration and unknown plasma samples, which is practically impossible in this case. A procedure to overcome these calibration difficulties is to apply second-order calibration [17] from excitation–emission matrix (EEM) fluorescence. In this experimental procedure, for each sample a matrix of data is obtained and a three-way arrangement is formed from several samples. By using *N*-way or second-order chemometric methods, quantitative analyses can be performed in the presence of unidentified interferences or in cases when there are compounds which are not present in all samples. Only the species of interest must be the same in the calibration standards and the samples to be analyzed. Qualitative analysis can be also performed, resulting in spectral deconvolution used for a better understanding of the system.

Several methods and algorithms have been proposed to be applied in second-order data sets, based on direct algebraic solutions such as TLD or GRAM [18] or on iterative procedures such as parallel factor analysis (PARAFAC) [19], MCR [20] or N-PLS [21]. The methods based on iterative algorithms have been most widely employed because they are less sensitive to instrumental noise and model deviations, opening a large number of practical applications in HPLC-spectroscopy [22], flow injection analysis [23] and tandem MS [24]. Also there are several applications with excitation–emission matrix fluorescence, including environmental monitoring [25–27], analysis of biological samples [28–30] and quantitation of drugs [31].

In this paper, a method for determination of doxorubicin in human plasma based on EEM fluorescence measurements is proposed and validated by its figures of merit. PARAFAC was employed for EEM spectra deconvolution and DXR quantitation. During the spectral deconvolution step, several procedures were used to determine the number of different fluorophores present in the data set, such as the split-half method, core consistency diagnostic (CORCONDIA) and residual analysis. All procedures converged to

the same number of two components. One component was identified as doxorubicin and the other as the sum of several fluorescence species of the plasma. In PARAFAC quantitation, the sample factor loadings were used to establish a linear relationship with DXR concentration and good results were obtained for samples at low mg l^{-1} concentrations. Also N-PLS was employed for DXR quantitation and cross-validation was used to find the optimum number of factors. The optimum number of factors was two and better results in relation to PARAFAC were obtained.

2. Theory

2.1. EEM fluorescence

In dilute solutions, the emission fluorescence intensity I, obtained at several excitation–emission measurements for many fluorescing species in a sample, can be describe as

$$I_{ij} = \sum_{f=1}^{F} a_f \delta_{fi} \varepsilon_{fj} \quad (1)$$

where I_{ij} is the measured intensity at the emission i and excitation j wavelengths; a_f the concentration of the fth fluorophore; δ_{fi} the relative emission coefficient at the emission wavelength i of the fth fluorophore; ε_{fj} the molar absorptivity coefficient at the excitation wavelength j of the fth fluorophore; F is the number of fluorophores in the sample.

For many samples containing several different fluorophores, Eq. (1) can be written as matrix products:

$$\boldsymbol{F} = \boldsymbol{A}(\boldsymbol{C}| \otimes |\boldsymbol{B})^{\mathrm{T}} \quad (2)$$

where $\boldsymbol{A}$ is the matrix of emission spectral profile of all fluorescing species at all measured wavelengths; $\boldsymbol{B}$ is a concentration matrix of all fluorescing species; $\boldsymbol{C}$ is the matrix of absorption spectral profiles of all fluorescing species at all measured wavelengths; $|\otimes|$ is the Katri-Rao product.

All terms involved into the fluorescence equation have linear independence, making a perfectly trilinear profile model. However, the presence of elastic Rayleigh scatter at a specific EEM region produces non-linear profiles, not related to species fluorescences. If a trilinear model is intended to be adjusted, these non-linear regions should be replaced by missing values.

2.2. PARAFAC

Parallel factor analysis (PARAFAC) is a decomposition method for N-way data proposed by psychometricians in the seventies and used since the nineties by chemists [32]. A PARAFAC model of a three-way array is given by three loading matrices, $\boldsymbol{A}$, $\boldsymbol{B}$ and $\boldsymbol{C}$, with elements a_{if}, b_{jf} and c_{kf} (Eq. (3)), respectively. The trilinear model is found to minimize the sum of squares of the residuals, e_{ijk}, in the model.

$$x_{ijk} = \sum_{f=1}^{N} a_{if} b_{jf} c_{kf} + e_{ijk} \quad (3)$$

where x_{ijk} is an element of the trilinear data set.

The algorithm used to solve the PARAFAC model is alternating least squares (ALS). ALS successively assumes the loadings in two modes and then estimates the unknown set of parameters of the last mode. In some instances, constraints are used to help algorithm convergence and the physical meaning of the loadings.

PARAFAC can be considered a constrained version of the more general method Tucker3 [32] with a super-identity core matrix. It is less flexible, uses fewer degrees of freedom, and provides unique solutions that are not dependent on rotation. This last feature is a great advantage for the modeling of spectroscopic data. On the other hand, this is also a problem, because initial knowledge about the underlying factors is required. For certain systems, only the experimental analyst's knowledge or techniques such as split-half analysis [33] or estimation of the core consistency [32] have been shown to be efficient. In the split-half experiments, one type of jack-knife validation [34], the data set is split into several sub-blocks and then PARAFAC is performed on each sub-block. Identical loadings on sub-blocks will be obtained if the correct number of factors (fluorophores) was chosen, due to the uniqueness of the PARAFAC model. The core consistency diagnostic indicates how well the model is in concert with the distribution of superdiagonal and off-superdiagonal elements of the Tucker3 core. If the PARAFAC model is correct, then it is expected that the superdiagonal elements will be close to one and

the off-diagonal elements close to zero. The core consistency diagnostic (CORCONDIA) is defined as

$$\text{CORCONDIA} = 100 \times \left(1 - \frac{\sum_{d=1}^{F}\sum_{e=1}^{F}\sum_{f=1}^{F}(g_{def} - t_{def})^2}{\sum_{d=1}^{F}\sum_{e=1}^{F}\sum_{f=1}^{F}t_{def}^2}\right) \quad (4)$$

where g_{def} is the calculated element of the core using the PARAFAC model, defined by dimensions ($d \times e \times f$); t_{def} the element of a binary array with zeros in all elements and ones in the superdiagonal (the expected Tucker3 core) and F is the number of factors in the model. In an ideal PARAFAC model, g_{def} is equal to t_{def} and, in this case, CORCONDIA will be equal to 100%.

PARAFAC can be also used for quantitation. The sample loadings are fitted against the known concentration of a calibration set and new samples can be analyzed using the model developed in the calibration phase.

2.3. N-way regression—N-PLS

Partial least squares regression [16] is a supervised method for building regression models between sets of pairs: independent (called X) and dependent variables (called Y). Multi-linear PLS (N-PLS) [21] is an extension of the two-way PLS algorithm for cases where the independent set is an array of higher order than two. As with PLS, the aim is to find components in the multidimensional array, that have maximum covariance with the dependent variables. In the case of excitation–emission fluorescence calibration, the independent set is a three-way array formed by excitation–emission fluorescence measurements of several samples and the dependent set is a vector of concentrations, explained by the argument:

$$\max_{w_a^J, w_a^K}\left[\text{cov}(\boldsymbol{t}_a, \boldsymbol{y})|\min\left(\sum_{i=1}^{I}\sum_{j=1}^{J}\sum_{k=1}^{K}(x_{ijk} - t_{a,i}w_{a,j}^J w_{a,k}^K)^2\right)\right] \quad (5)$$

where $\boldsymbol{y}$ ($I \times 1$) is the concentration vector; $\boldsymbol{t}_a$ ($I \times 1$) the PLS scores and $\boldsymbol{w}_a^J$ ($J \times 1$) and $\boldsymbol{w}_a^K$ ($K \times 1$) are the PLS weight vectors for the ath model factor. The factor term is called latent variable in bidimensional PLS.

Unlike PARAFAC, the choice of the number of factors is not performed directly from the number of fluorescing species present and more or fewer factors than the number of fluorophores can be chosen. This larger number of factors can be necessary to explain non-linearities such as quenching, Rayleigh scatter and missing values, whereas a lesser number of factors can be found in the presence of highly correlated fluorophores species in the studied system. An adequate choice of the factor number makes a suitable modeling without over fitting and a lack of trilinearity is not considered critical, as the main aim in the model is to find a subspace in X which can be used for regression. It has been shown in the literature that multi-linear regression methods can work well even on data with no strict multi-linear structure. The most employed method to find the adequate number of factors is cross-validation with the leave-one-out procedure [16] where, from the calibration samples, one sample is left out and the model is developed using different numbers of factors. The concentration for the sample that did not participate in model development is predicted with several factor numbers and, from comparison with the true valor, an error is estimated for each factor number employed. This procedure is repeated for all calibration samples and a mean error is calculated. The number of factors that produced the least error within a threshold value is then chosen.

2.4. Figures of merit

Alternatives methodologies need to be validated by comparison with other established methods. The most important process for comparison of analytical methods is the determination of figures of merit, such as sensitivity, selectivity and limit of detection (L_D). In multivariate calibration, the net analyte signal (NAS) calculation [35] is strictly necessary for the FOM evaluation. The NAS for multi-way data is analogous to those for first-order procedures, which is defined as the part of the signal that relates uniquely to the analyte of interest. In this case, as the data is bilinear, the NAS is the pure analyte data obtained by PARAFAC [36]. The sensitivity is estimated as the NAS at unit concentration, as shown in Eq. (6), and the selectivity

is the ratio between the sensitivity and the total signal, as shown in Eq. (7).

$$\mathrm{SEN} = ||\mathbf{NAS}||_F \tag{6}$$

$$\mathrm{SEL} = \frac{||\mathbf{NAS}||_F}{||\boldsymbol{N}||_F} \tag{7}$$

where **NAS** is a matrix with dimensions 56 × 282; $\boldsymbol{N}$ is the matrix of the total signal and $||\cdot||_F$ is the Frobenius norm.

For N-PLS the sensitivity is calculated as for first-order calibration, i.e. the inverse of the norm of vector of regression coefficients. In this case, the matrix of coefficients of regression generated by N-PLS are transformed to a vector. Multiplying this parameter by analyte concentration gives the NAS. From NAS it is possible to calculate the selectivity by Eq. (7).

The limit of detection (L_D) [30] is calculated as

$$L_D = 3.3s(0) \tag{8}$$

where $s_{(0)}$ is the standard deviation in the concentration estimated for three different blank samples, in the PARAFAC and N-PLS models.

3. Experimental

3.1. Apparatus

The samples were measured on a Perkin-Elmer LS 55 Luminescence Spectrometer with a 10 mm quartz cuvette at 23 ± 1 °C. The FL WinLab Software (Perkin-Elmer) was used for measurements, and the spectra were imported to Matlab version 6.1, using a homemade program. The *N*-way toolbox for Matlab version 2.1 [37], available at http://www.models.kvl.dk/source, was employed for PARAFAC and N-PLS calculations. All programs were run on an AMD Thunderbird 1.3 GHz microprocessor IBM compatible microcomputer.

3.2. Reagents and solutions

Doxorubicin hydrochloride was obtained as a crystalline powder from Instituto de Tecnologia do Paraná (TecPar), Brazil. A stock solution with a concentration of 150 μg ml^{-1} was prepared by dissolving the doxorubicin hydrochloride in water and stored in glass at −20 °C, protected from light, for a maximum period of 1 week.

Deionized water (Millipore) was used in all experimental preparations. All glassware used were previously soaked in 10% (v/v) HNO_3 for 62 h and rinsed with distilled and deionized water.

3.3. Samples

Ten blood samples were obtained from healthy volunteers at the Clinical Hospital of Campinas State University, Brazil. On the same day, the samples were centrifuged for 20 min at 3500 rpm and 3.0 ml of supernatant were transferred to a clean vacuum tube and stored at −20 °C until the experiments were performed.

3.4. Procedure

DXR usually is injected as a dose of 60–75 mg m^{-2}, giving an initial concentration of about 20 μg ml^{-1} in an adult male. Only a fraction of this injected drug will be present in the plasma. Therefore, we decided to work in concentrations not superior to 50% of the initial dose. The experimental points were studied with different concentrations of DXR in the range of 0.75–11.25 μg ml^{-1}. These points were made from the appropriate addition of the stock solution of doxorubicin into 2 ml of plasma directly in the quartz cuvette, homogenized with a micro-magnetic bar. The EEM spectra were recorded at excitation wavelengths from 390 to 500 nm at regular steps of 2 nm and the emission wavelengths from 510 to 650 nm at 0.5 nm steps. The excitation and emission monochromator slit widths were 10 nm and a scanning rate of 900 nm min^{-1} was used. For each sample a matrix of fluorescence intensities with dimensions 56 × 282 (excitation wavelengths × emission wavelengths) was obtained.

4. Results and discussion

4.1. Natural fluorescence of human plasma

A three-dimensional plot of an EEM fluorescence of human plasma is presented in Fig. 2(a). It is possible to observe that there are two main bands, one

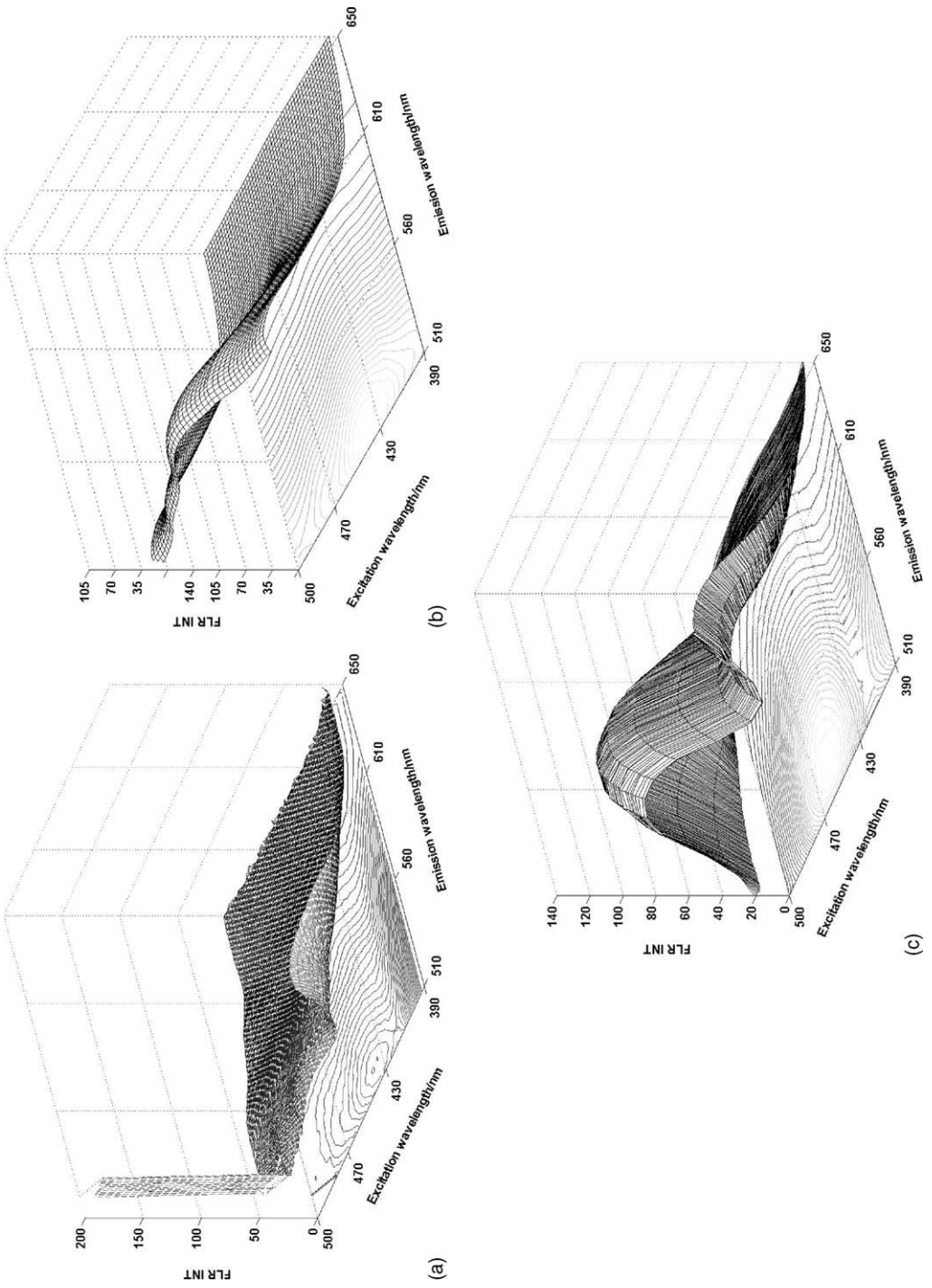

Fig. 2. Typical fluorescence excitation–emission spectrum of (a) human plasma, (b) bilirubin and (c) riboflavin.

at excitation/emission wavelengths around 450 nm/515 nm and another at an excitation wavelength near to 390 nm and emission wavelength around 515 nm. By comparison with the excitation–emission profiles of species normally present in the plasma, the peaks observed can be attributed mainly to bilirubin (Fig. 2(b)) and riboflavin (Fig. 2(c)).

Rayleigh scatter in the range of 490–500 nm excitation wavelengths and at 510–520 nm emission wavelengths is also observed. The Rayleigh scatter is not related to trilinear EEM fluorescence and these areas were replaced by missing values. When using the *N*-way toolbox developed by Andersson and Bro [37], the missing values are initially replaced by random elements. After each iteration a model is calculated, and the missing values are replaced with the model estimates. It is very important to note that the elements in this triangular part of the matrix holding the data of each sample cannot be replaced with zeros. Even though emission values below the Rayleigh area are approximately zero because fluorescence below the excitation wavelengths does not exists, this part does not conform to the trilinear model. Therefore, a PARAFAC model using all experimental data would be prone to some instability in this area.

5. PARAFAC

5.1. Number of factors

When using PARAFAC, a initial definition of the number of factors to build the model is necessary. This choice is of fundamental importance because all conclusions about the deconvolution and quantitation results will be related with this number of factors.

In PARAFAC, it is possible to use several constraints such as non-negativity, unimodality or orthogonality. In this work an unconstrained model was preferred as more realistic results can be obtained, because in fluorescence the structural model in itself should be unique. Orthogonality is not applicable for spectral data and, based on prior knowledge, it is known that the spectra are not unimodal. Only non-negativity could be tried, but no improvement was observed when it was applied in relation to an unconstrained model.

Unconstrained PARAFAC models of the EEM data were developed using one to five components and the percentage of fit was used as the initial approach to select the number of factors. The percentage of fit value corresponds to how well the model can reproduce the experimental data and it is given as

$$\text{fit}\,(\%) = 100 \times \left(1 - \frac{\sum_{i=1}^{I}\sum_{j=1}^{J}\sum_{k=1}^{K}(x_{ijk} - \hat{x}_{ijk})^2}{\sum_{i=1}^{I}\sum_{j=1}^{J}\sum_{k=1}^{K}x_{ijk}^2}\right) \quad (9)$$

where x_{ijk} is the ijkth experimental element and $\hat{x}_{ijk}$ the ijkth element predicted by the model. This operation is only performed with non-missing values in the EEM fluorescence data, since no calculations were possible with missing-values. In this case, first the PARAFAC model was developed using missing-values and for percentage of fit estimation, zeros were placed in substitution of the missing-values.

The results are presented in Table 1. It is possible to note that this parameter is not conclusive for selection of the number of factors, since percentage of fit higher than 99% were obtained using from 2 to 5 factors. This parameter is important to identify if there are factors lacking in the model. Therefore, other more conclusive tools, such as CORCONDIA and split-half analysis, were used in this study.

5.2. Core consistency diagnostic (CORCONDIA)

All data set ($10 \times 56 \times 282$) was utilized for the core consistency evaluation, using one to five factors, with the values calculated according to Eq. (4). The results are also shown in Table 1. The analysis using CORCONDIA indicates that two factors are necessary, because the utilization of more factors leads to a great decrease of the core consistency and hence of the trilinearly of the data modeled. Two factors give a CORCONDIA value of 100% (a perfect trilinear model)

Table 1
Fit (%) and core consistency diagnostic (CORCONDIA) for PARAFAC models using 1–5 factors

Number of factors	1	2	3	4	5
Fit (%)	94.77	98.75	99.39	99.68	99.86
CORCONDIA (%)	100	100	0.83	2.78	0.59

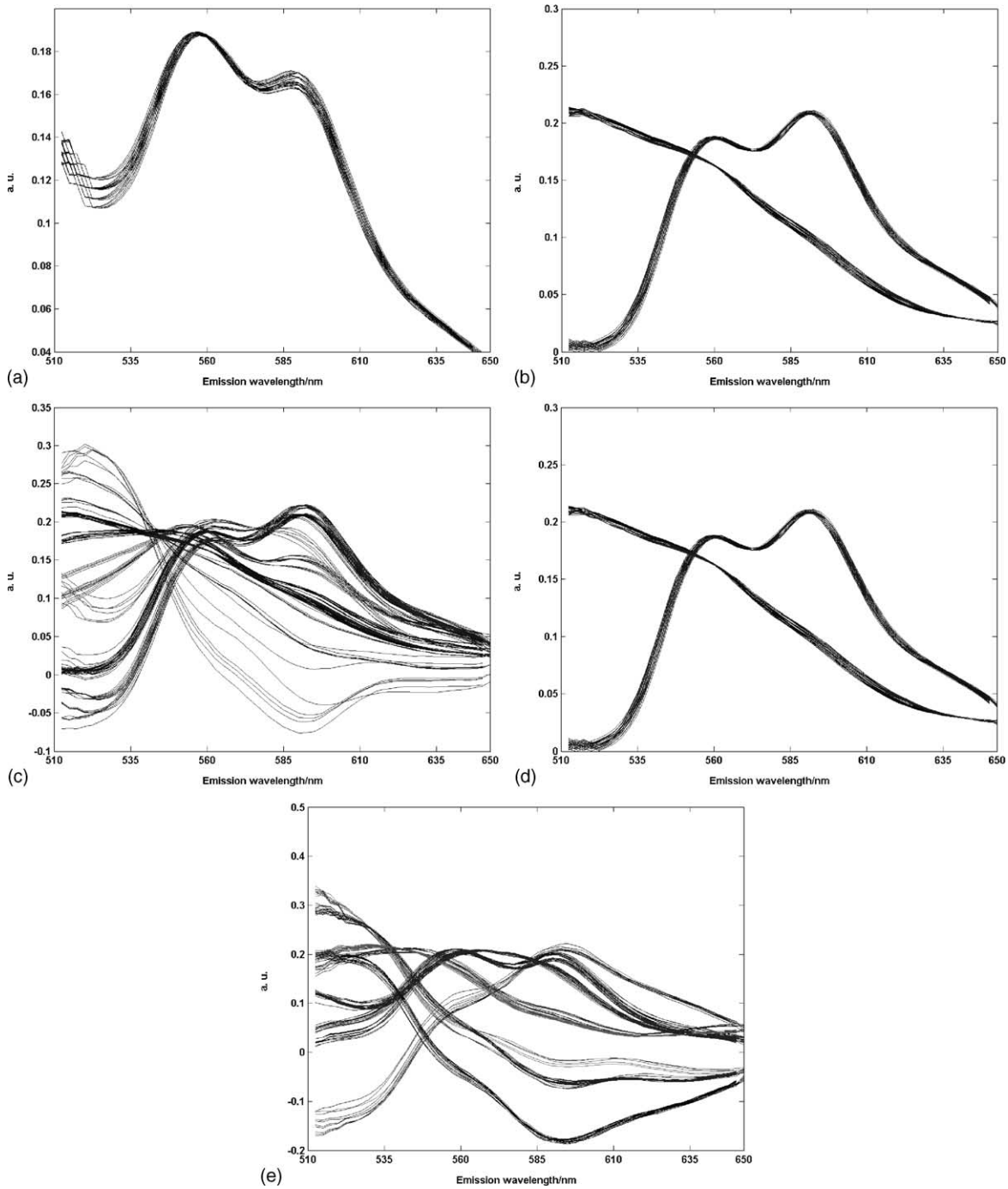

Fig. 3. Split-half procedures: (a) using one factor, (b) two factors, (c) three factors, (d) four factors and (e) five factors.

whilst, when using three or more factors, this value diminishes to values below to 3%.

5.3. Split-half analysis

Firstly, the fluorescence data with ten samples (dimension $10 \times 56 \times 282$) was split into four groups, named A, B, C and D, where each one had five samples and same an equal of excitation and emission wavelengths (new dimension for each group: $5 \times 56 \times 282$). Set A consisted of the first half of the samples and set B the last half. Set C was created from the first three samples of set A and the last two of B. While set D consisted of the last two samples from A and the first three of B.

Each original group (A, B, C and D) was divided into 25 parts with dimensions: $(5 \times 12 \times 57)$, $(5 \times 12 \times 56)$, $(5 \times 11 \times 57)$ or $(5 \times 11 \times 56)$, generating 100 new sets. In the next step, 100 unconstrained PARAFAC models were developed to appraise the loading similarities. Fig. 3 shows the PARAFAC results using 1–5 factors for the mode related to the emission spectra. Only when two factors were used did all 100 models of subset converge to the same result. These results confirm that two factors are most adequate, since for a higher number of factors the loading vectors diverge considerably, depending on the subset used.

Therefore, both split-half analysis and core consistency indicated the use of two factors for deconvolution. Chemically, two factors are a suitable conclusion because the EEM has two patterns: the fluorescence of doxorubicin and the inherent fluorescence of human plasma. Certainly, several fluorophores are present in the plasma but if they are similar, the PARAFAC model will not interpret them as independent factors.

5.4. Deconvolution and calibration

As presented in Section 5.3, two factors for the unconstrained PARAFAC model furnished the best model for the deconvolution of data and two triads were obtained after decomposition. Each triad consisted of three orthogonal loadings, composed by concentration × excitation wavelength × emission wavelength. Fig. 4 shows the results obtained, where one factor is clearly related to DXR, as confirmed by comparison with the excitation–emission spectra of the pure drug, presented in Fig. 5. Another factor

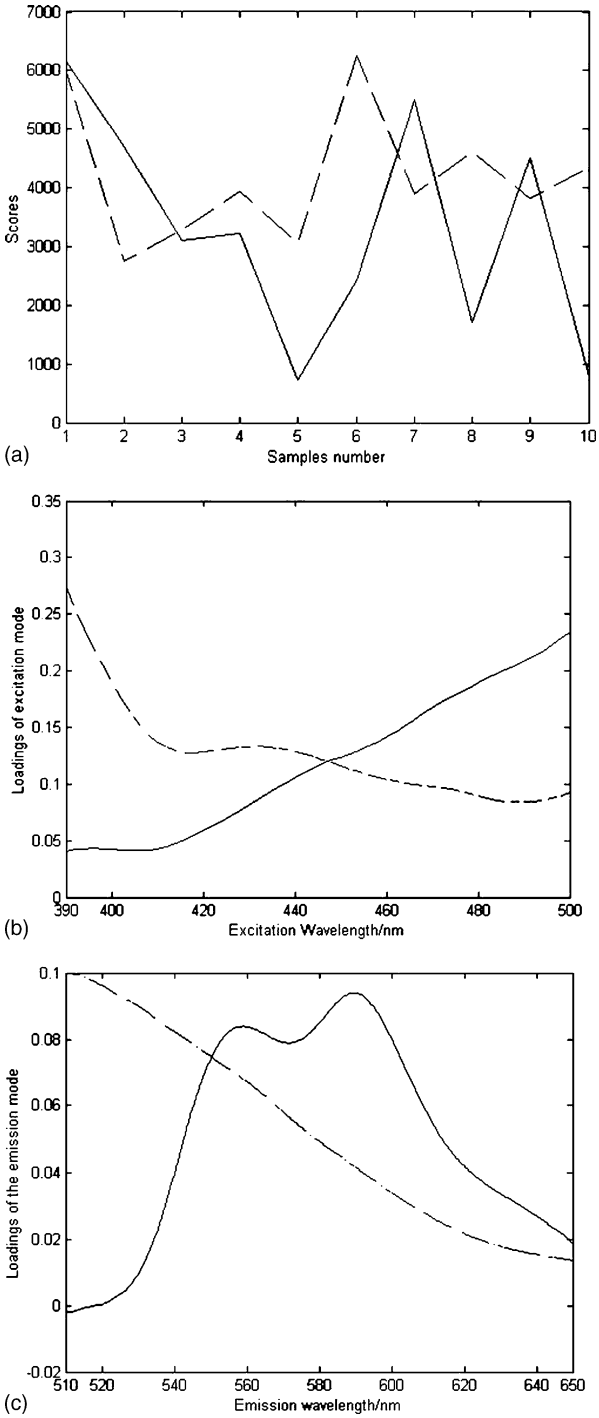

Fig. 4. PARAFAC decomposition using two factors ((- - -) plasma and (—) DXR): (a) sample mode, (b) excitation mode and (c) emission mode.

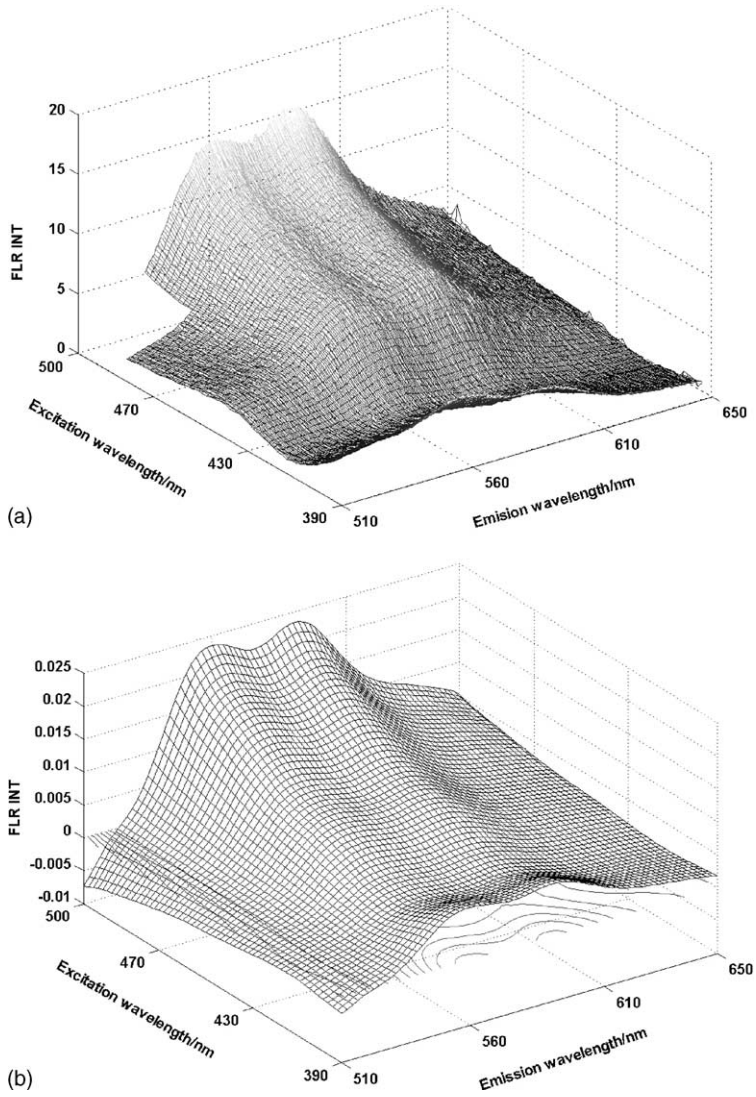

Fig. 5. (a) Excitation–emission spectrum of pure DXR and (b) excitation–emission spectra of PARAFAC recovered first factor.

is not considered a fluorescence of a single analyte, but it is related to a mixture of plasma constituents, such as bilirubin and riboflavin. Fig. 6 shows the emission–excitation profile of this factor. It is possible to observe that this profile is very similar to that presented in Fig. 2(a), the inherent EMM fluorescence of plasma. A possible explication for these results is that bilirubin and riboflavin excitation–emission profiles are similar and PARAFAC did not resolve these chemical species into separated factors.

The PARAFAC loadings of concentration mode (scores) associated with DXR were used to establish a linear relationship with DXR concentration, generating a calibration model. A cross-validation procedure with leave-one-out samples was performed to verify calibration model viability. In this procedure, ten models were developed with one different prediction sample at a time and in all of them good regression curves were obtained (regression coefficients higher than 0.95). A root mean square error

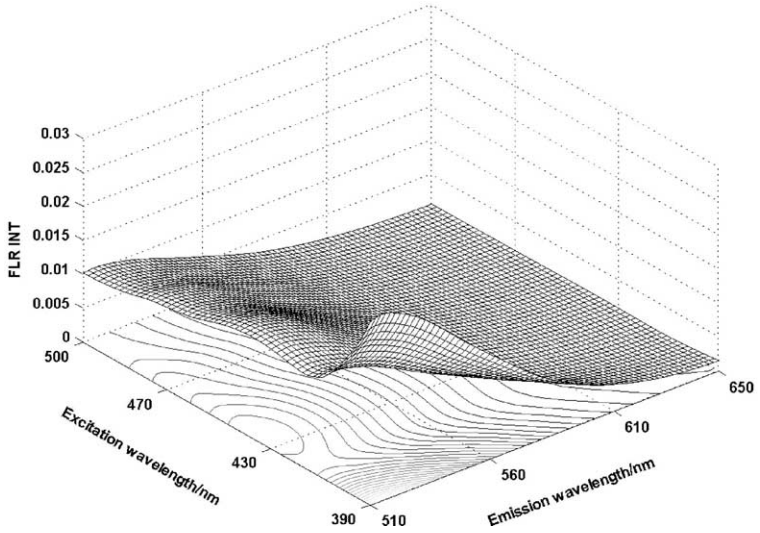

Fig. 6. Excitation–emission profile of the second PARAFAC factor.

of cross-validation (RMSECV) of 0.060 μg ml^{-1} and a mean relative error of prediction of 4.4% were obtained. These results indicate that it is possible to quantify DXR in human plasma using the PARAFAC scores.

In this application, we have observed that the plasma constituents cause quenching in the fluorescence emission. Our first attempts were to built a calibration model using samples of DXR prepared in water. By using the second order advantage, DXR in plasma would be predicted from the calibration curve developed in water. However, fluorescence emission of DXR in water is greater than in plasma and the model failed. Only when using all calibration samples in plasma was a feasible model developed. A possible alternative would be to dilute the plasma samples to avoid the quenching effects, but this procedure can produce an increase in detection limits, for example.

5.5. N-PLS

In the N-PLS calculations, a cross-validation with leave-one-out procedure was adopted to find the best number of latent variables (factors) to be used. Table 2 shows the explained variance for both *X* and *Y* blocks using 1–5 factors. Based on the results, two factors were chosen because they produced the lowest error of prediction and described practically all data variance in the *X* and *Y* blocks. Using two factors, a mean square error of cross-validation of 0.045 μg ml^{-1} and a mean relative error of prediction of 2.0% were obtained.

These better results of N-PLS, in relation to PARAFAC, must to be interpreted with caution, because only 10 samples were used to calculate the errors. However, these results can be explained because in N-PLS the algorithm is optimized to establish a relationship between the fluorescence spectra and DXR concentrations, and other sources of variations or noise are not incorporated into the model.

5.6. Figures of merit

A RMSECV of 0.060 μg ml^{-1} and a mean relative error of prediction of 4.4% were obtained for DXR determination using PARAFAC and a RMSECV of 0.045 μg ml^{-1} and a mean relative error of prediction of 2.0% for N-PLS. Table 3 presents other figures of merit such as sensitivity, selectivity, limit of detection and precision, expressed as the repeatability (three

Table 2
Explained variance for *X* and *Y* blocks

Number of factors	1	2	3	4	5
X block (%)	73.13	95.73	97.73	98.09	99.67
Y block (%)	88.95	99.57	99.98	100.00	100.00

Table 3
Analytical figures of merit

Figures of merit	PARAFAC	N-PLS
Sensitivity (FLR[a] ml μg^{-1})	380	270
Selectivity	0.49	0.70
Limit of detection ($\mu g\,ml^{-1}$)	0.032	0.032
Precision (%)	2.0	2.0

[a] FLR is the fluorescence intensity (arbitrary units).

concentrations/three replicates). As can be observed, the figures of merit for both PARAFAC and N-PLS are very similar and only the selectivity of N-PLS is greater than that of PARAFAC.

These results can be compared with other methods developed for DXR determination. There are methods based on HPLC separation with ES–MS detection [6] and based on capillary electrophoresis with laser-induced fluorescence detection [9] that present limits of detection on the order of 0.001 $\mu g\,ml^{-1}$. Also, there are methods based on UV-Vis detection [12] and Raman detection [13], whose detection limits are in the range of 0.034–0.42 $\mu g\,ml^{-1}$. The EMM fluorescence/chemometric approach presented in this paper can be successfully compared with these methods. The other separation methods, based on very sensitive detection, present lower detection limits. However, they all require sample pretreatment procedures and separation steps prior to detection.

6. Conclusions

This work demonstrated that the use of excitation–emission matrix fluorescence and multi-way analysis is a powerful tool for complex analysis of drugs in plasma since, in most cases, these compounds present fluorescence.

Deconvolution using PARAFAC resulted in two factors, one due the DXR and other due to two plasma constituents. It was demonstrated that the conjunction of several procedures such as percentage of fit, CORCONDIA and split-half analysis lead to a more realistic estimation of the number of factors in a PARAFAC model.

The figures of merit calculated for both PARAFAC and N-PLS were very similar and the results should be considered satisfactory based on the complexity of the samples analyzed. They are acceptable for some real applications, such as pharmacokinectic investigations in cancer patients.

Acknowledgements

The authors wish to thank the CNPq for a fellowship to M.G. Trevisan, FAPESP (proc. 1999/12124-7), Clinical Hospital of Campinas State University, Brazil and the anonymous volunteers that provide the blood samples.

References

[1] F. Arcamone, G. Cassineli, G. Fantini, A. Grein, P. Orezzi, C. Pol, C. Spalla, Biotechnol. Bioeng. 11 (1969) 1101.
[2] United States Pharmacopoeia XXI, Rockville, MD, USA, 1994, p. 357.
[3] G.N. Hortobagyi, Drugs 54 (Suppl. 4) (1997) 1.
[4] G. Zagotto, B. Gatto, S. Moro, C. Sissi, M. Palumbo, J. Chromatogr. B 764 (2001) 161.
[5] S. Fogli, R. Danesi, F. Innocenti, A. Di Paolo, G. Bocci, C. Barbara, M. Del Tacca, Ther. Drug Monit. 21 (1999) 367.
[6] F. Lachâtre, P. Marquet, S. Ragot, J.M. Gaulier, P. Cardot, J.L. Dupuy, J. Chromatogr. B 738 (2000) 281.
[7] J. van Asperen, O. Van Tellingen, J.H. Beijnen, J. Chromatogr. B 712 (1998) 129.
[8] Q. Zhou, B. Chowbay, J. Pharm. Biomed. Anal. 30 (2002) 1063.
[9] T. Perez Ruiz, C. Martinez Lozano, A. Sanz, E. Bravo, Electrophoresis 22 (2001) 134.
[10] N.J. Reinhoud, U.R. Tjaden, H. Irth, J. van der Greef, J. Chromatogr. B 574 (1992) 327.
[11] A. Gavenda, J. Sevcik, J. Psotova, P. Bednar, P. Bartak, P. Adamovsky, V. Simanek, Electrophoresis 22 (2001) 2782.
[12] C.S.P. Sastry, J. Rao, Talanta 43 (1996) 1827.
[13] A. Loren, C. Eliasson, M. Josefson, K.V.G.K. Murty, M. Käll, J. Abrahamsson, K. Abrahamsson, J. Raman Spectrosc. 32 (2001) 971.
[14] O.S. Wolfbeis, M. Leiner, Anal. Chim. Acta 167 (1985) 203.
[15] S. Madhuri, S. Suchitra, P. Aruna, T.G. Srinivasan, S. Ganesan, Med. Sci. Res. 27 (1999) 635.
[16] H. Martens, T. Naes, Multivariate Calibration, Wiley, New York, 1989.
[17] A.R. Muroski, K.S. Booksh, M.L. Myrick, Anal. Chem. 68 (1996) 3534.
[18] S. Li, J.C. Hamilton, P.J. Gemperline, Anal. Chem. 64 (1992) 599.
[19] R. Bro, Chemom. Intell. Lab. Syst. 38 (1997) 149.
[20] M. Esteban, C. Ariño, J.N. Díaz-Cruz, M.S. Díaz-Cruz, R. Tauler, Trend Anal. Chem. 19 (2000) 49.
[21] R. Bro, J. Chemom. 10 (1996) 47.

[22] H.L. Wu, M. Shibukawa, K. Oguma, J. Chemom. 12 (1998) 1.
[23] J. Saurina, S. Hernandez-Cassou, R. Tauler, Anal. Chim. Acta 312 (1995) 189.
[24] C.G. Zampronio, S.P. Gurden, L.A.B. Moraes, M.N. Eberlin, A.K. Smilde, R.J. Poppi, Analyst 127 (2002) 1054.
[25] J. Saurina, C. Leal, R. Compañó, M. Granados, R. Tauler, M.D. Prat, Anal. Chim. Acta 409 (2000) 237.
[26] R.D. Jiji, G.G. Andersson, K.S. Booksh, J. Chemom. 14 (2000) 171.
[27] R.D. Jiji, G.A. Cooper, K.S. Booksh, Anal. Chim. Acta 397 (1997) 72.
[28] R. Bro, Chemom. Intell. Lab. Syst. 46 (1999) 133.
[29] R.P.H. Nikolajsen, A.M. Hansen, R. Bro, Luminescence 16 (2001) 91.
[30] A.M. de la Peña, A.E. Mansilla, D.G. Gómez, A.C. Olivieri, H.C. Goicoechea, Anal. Chem. 75 (2003) 2640.
[31] J.C.G.E. Silva, J.M.M. Leitão, F.S. Costa, J.L.A. Ribeiro, Anal. Chim. Acta 453 (2002) 105.
[32] R. Bro, Multiway Analysis in the Food Industry: Models, Algorithms and Applications, Doctoral dissertation, University of Amsterdam, Amsterdam, 1998.
[33] M.M. Reis, D.N. Biloti, M.M.C. Ferreira, F.B.T. Pessine, G.M. Teixeira, Appl. Spectrosc. 55 (2001) 847.
[34] J. Riu, R. Bro, Chemom. Intell. Lab. Syst. 65 (2003) 35.
[35] A. Lorber, K. Faber, B.R. Kowalski, Anal. Chem. 69 (1997) 1620.
[36] K.S. Booksh, B.R. Kowalski, Anal. Chem. 66 (1994) 782A.
[37] C.A. Andersson, R. Bro, Chemom. Intell. Lab. Syst. 52 (2000) 1.